

Effects of Additives on Anatase to Rutile Phase Transformation of TiO₂ Powder Synthesized by Sol–Gel Route

N. BELABED^{a,*}, A. CHARI^a, A. AYADI^b,
K. BOUSSNINA^a AND S. KASOUIT^c

^a*Semiconductor physico-chemistry laboratory, Department of Physics, University Frères Mentouri Constantine 1, Algeria*

^b*Laboratory of Microstructure and Defects in Materials, Department of Physics, University Frères Mentouri Constantine 1, Algeria*

^c*Lam Research Corporation 4300 Cushing Parkway 94538, Fremont, California USA*

Received: 13.01.2022 & Accepted: 13.04.2022

Doi: [10.12693/APhysPolA.142.226](https://doi.org/10.12693/APhysPolA.142.226)

*e-mail: manel.th78@gmail.com

The titanium oxide (TiO₂) powders were synthesized by a sol–gel route with TiCl₄ as a precursor and at ambient conditions. The powders have been dried up at 100°C for 12 h and annealed for 1 h at temperatures between 400 and 800°C. In the present work, the effects of dissolved ions (e.g., Na⁺, Cl[−], and F[−]) on the structural particle morphology were investigated using various additives, such as NaCl, NaOH, HCl, and HF. The powders were analyzed by X-ray diffraction and Raman spectroscopy, and the scanning electron microscopy technique was used for agglomerate observations. The photocatalytic activities of the TiO₂ powders were evaluated using the degradation reaction of methylene blue. The results show that the presence of Na⁺ accelerates the transition from anatase to rutile, while that of Cl[−] and F[−] delays this transition. The additives modify the pH of the solution and, as a result, the size of the spherical agglomerates constituted of nanoparticles crystalline. These agglomerates are constituted of grains, the size of which depends on the temperature. A more acid solution leads to smaller agglomerates of 0.5 μm size, while a solution that is more basic gives bigger agglomerates. The better photoactivity is obtained in an anatase/rutile mixture with a high fraction of the rutile. Na⁺ in the TiO₂ films affects photocatalytic activity. The surface states on the metal oxide have a considerable influence on the photocatalytic activity with varying pH.

topics: TiO₂ nanoparticles, sol–gel method, anatase–rutile phases, photocatalytic activity

1. Introduction

TiO₂ is a semiconductor metal oxide inert with a gap near UV, which can be synthesized with different methods (sol–gel, CVD, PVD...). It attracts much interest thanks to its wide range of applications in photocatalysts [1], electrochemical solar cells [2], pigments and gas sensors [3, 4]. The most important point in our study is photocatalysis. Titanium dioxide, TiO₂, is an important photocatalytic material that exists as two main polymorphs, anatase and rutile. The structure of the TiO₂ phase differs only in the mode of association of TiO₆ octahedral, which can be connected to each other by edges, in the case of rutile, and/or vertices, in the case of anatase.

The presence of either or both of these phases influences the photocatalytic performance of the material. There are many studies on the photocatalytic activity of TiO₂ in its different phases [5, 6]. It was observed that anatase is more efficient as a photocatalyst than rutile [7], and pure rutile is rarely

active for the photodegradation of organic species in aqueous solutions [8, 9]. However, some works have indicated that rutile titania can possess high photocatalytic activity [10, 11]. Anatase to rutile phase transformation in TiO₂ is an area of both scientific and technological interest [12, 13]. Annealing temperature has a strong influence on the phase transformation of TiO₂ anatase transforming to rutile under calcination, typically between 600 and 700°C [14]. In this paper, we report on the preparation of nanocrystalline TiO₂ using the sol–gel method and discuss the effects of annealing temperature and additives on the anatase to rutile phase transformation. We compared the effect of the additives on the photocatalytic activity of TiO₂.

2. Materials and methods

Nanocrystalline TiO₂ powders were synthesized by the sol–gel method. The sol was formed by dissolving 10 ml of titanium tetrachloride (TiCl₄) of 98% purity in 200 ml of deionized water with

Stationary pH for synthetic solutions containing TiCl_4 . TABLE I

Ion	pH
TiCl_4	-0.7
$\text{TiCl}_4 + \text{NaCl}$	-1.3
$\text{TiCl}_4 + \text{NaOH}$	13.5
$\text{TiCl}_4 + \text{HCl}$	-0.5
$\text{TiCl}_4 + \text{HF}$	+1

constant stirring, then 0.5 g citric acid was added to the reaction solution for slow release of Ti^{3+} ions. The solution was stirred for 30 min at ambient temperature, then dried at 100°C for 12 h in an oil bath and annealed for 1 h at temperatures ranging from 400 to 800°C . The pH of the solution was measured during the stirring time by pH meter electrodes (Thermo Scientific Orion Star and Star Plus meters). Additional TiO_2 powders were prepared using the same method, with additives (1 mol) such as NaCl, NaOH, HCl, and HF. The addition of additives allows the pH to be controlled over a very wide range, from -1.5 to 13 . The solutions were strong acids and were not diluted, which resulted in the concentration of hydrogen ions greater than 1 M, leading to negative pH values measured by a pH meter. The pH values of the solution with different types of additives used are shown in Table I. Xerogels containing alkaline have been washed several times with deionized water and filtered by filter paper.

The X-ray diffraction (XRD) patterns of the calcined powders were obtained with a PANalytical Empyrean X-ray diffractometer in the diffraction angle range $2\theta = 20\text{--}80^\circ$ using $\text{Cu } K_\alpha$ radiation. The anatase/rutile percentages were calculated from the resulting diffracted grams using the Spurr equation [15]

$$\% \text{rutile} = \left(1 + \frac{0.8 I_A(101)}{I_R(110)} \right)^{-1}. \quad (1)$$

where I_A is intensity of anatase peak and I_R is intensity of rutile peak. To reduce NaCl, the powders were washed with water and filtered. As NaCl and TiO_2 (rutile) have a common peak at $2\theta = 27.5^\circ$, we use the peak at 2θ located at 54.4° (211) to identify the rutile phase. The report $I_R(211) = 0.55I_R(110)$ has been used to obfuscate the filtering method.

Raman spectroscopy was employed as a technique secondary to XRD to confirm the above results and to determine the frequency of the Raman bands of anatase and rutile on each sample used. Raman spectra were obtained using a SENTERRA Raman spectrometer (Bruker). The morphology and microstructures were investigated by scanning electron microscopy (SEM) using VEGA TS 5130 MM (TESCAN).

To demonstrate the efficiency of photocatalytic degradation of TiO_2 powders, a solution of methylene blue (MB), (100 ml, 10 mg/l), was added

to 100 mg of crystallin TiO_2 and placed under UV light irradiation. The absorbance measurements were carried out with UV-VIS spectrophotometer (Shimadzu UV-1800) on a centrifuged solution of MB with TiO_2 powder. The concentration of the degraded methylene blue was calculated by the Beer-Lambert law, where the absorbance $A = \epsilon Cl$, ϵ is the molar absorption coefficient [$\text{M}^{-1} \text{cm}^{-1}$], l is the optical path length [cm], and C is the molar concentration [M].

3. Results and discussion

The X-ray diffraction measurement was used to investigate the effect of additives on the crystal structure of the synthesized TiO_2 nanocrystals. The XRD patterns of the nanoparticles of TiCl_4 , pure and with different additives (NaOH, NaCl, HCl, and HF), obtained by the sol-gel method at different calcination temperatures of 400 , 600 , and 800°C , are shown in Fig. 1a and 1b, c, d, and e, respectively. The diffraction patterns of pure powder synthesized at low temperatures show anatase phases (Fig. 1a). When temperature increased, we observed an important peak at 600°C corresponding to the (110) plane of rutile at $2\theta = 27.35^\circ$. The anatase-rutile transition begins at 600°C , as described in the literature [16]. This powder indicates the presence of a mixture of anatase and rutile phases. The anatase-rutile transition occurs at the lowest temperature ($< 600^\circ\text{C}$) for powders synthesized by adding NaOH or NaCl (see Fig. 1b and c). The presence of Na^+ ions accelerates the transition at low temperature. The percentage of rutile in the calcined sample is shown in Fig. 2. At room temperature the powder prepared with NaOH is 100% rutile and 60% for the one prepared by NaCl. The diffraction pattern of TiO_2 synthesized by the addition of HCl and HF (see Fig. 1d and e) does not exhibit clear peaks at ambient conditions, indicating that the powder is amorphous in nature. Powders synthesized with HCl and HF addition exhibit clear peaks of anatase phase at 400°C and 600°C . At 800°C , the XRD diagram presented one anatase peak (101), and the others disappeared, showing the texturization of the powders.

In Fig. 2 rutile peaks are not observed — the samples are 100% anatase. Anatase-rutile transition is influenced by impurities and dopants [16]. It has been suggested that Na^+ cations of small radius and low valence accelerate the transition to rutile owing to the increase in oxygen vacancies that result from the assumed substitution of Ti^{4+} ions with cations of lower valence [16]. Fluorine has the opposite effect, F^{-1} substitutes for O^{-2} , the anions charge balance requires the inclusion of two fluorine ions for each oxygen, Ti^{4+} vacancies appear and Fluorine has been reported to inhibit the phase transformation [17, 18]. The case of chlorine is more complex because it can not be a substitute for O^{-2} [18, 19].

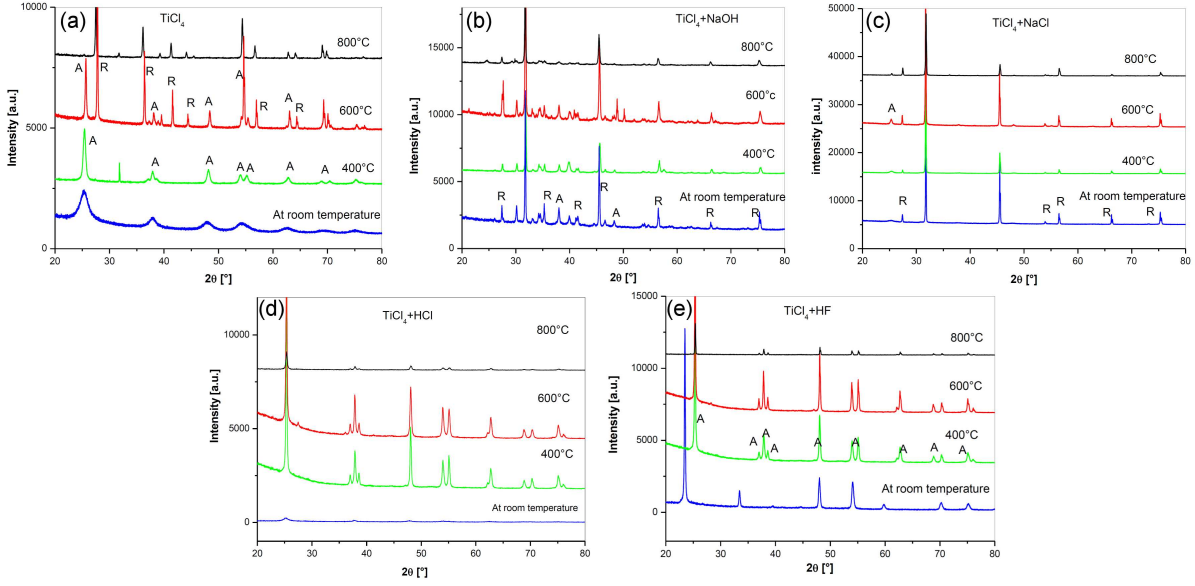


Fig. 1. XRD Pattern of the TiO₂ nanocrystals obtained from (a) TiCl₄, (b) TiCl₄+NaOH, (c) TiCl₄ + NaCl, (d) TiCl₄ + HCl and (e) TiCl₄ + HF.

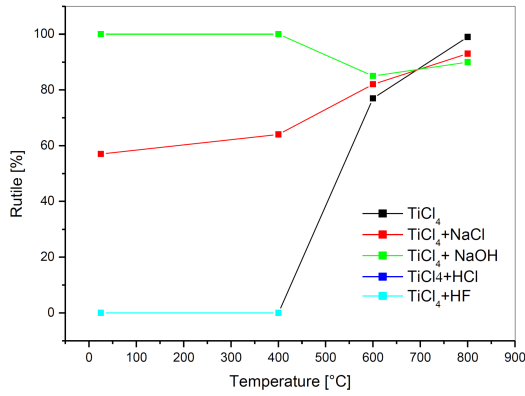


Fig. 2. Percentage of rutile in the calcined TiO₂ samples, determined by XRD for materials with different additives heated at different temperatures.

It has been observed that the addition of HCl delays the transition to rutile as we observed in our samples.

The average crystallite size of TiO₂ nanostructures was calculated using Debye–Scherrer’s equation

$$d = \frac{0.9\lambda}{\beta \cos(\theta)}, \quad (2)$$

where λ is the X-ray wavelength, θ is the Bragg diffraction angle, and β is the full to a half-maximum of the main peak in the XRD pattern. The changes in the crystallite sizes varied with annealing temperature and for samples with different additives, as presented in Fig. 3. The crystallite size of the powder synthesized at room temperature by the addition of NaCl and NaOH are similar, while the crystallite size of the rutile one, synthesized

under the same condition, is larger — in the range of 110–180 nm. It was suggested that the Na⁺ ion strongly affects the crystallite size of the anatase and rutile phases. In the case of the addition of HF and HCl, the crystallite size is small. When the annealing temperature increases, the size of the crystallite increases, up to a maximum at 600°C (phase transformation temperature). It is clearly shown that at this temperature the crystallite size is at the maximum for the two phases (anatase and rutile). The defects at the interface boundary of anatase are removed, leading to the conversion of the major fraction of anatase to rutile. Consequently, this reduces the stress field in this region, resulting in the release of lattice strain [19, 20]. At an annealing temperature over 600°C, the size of the smaller crystallite increases to the detriment of other, larger grains of both phases. This leads to a decrease in the average crystallite size, which at 800°C is about 60 nm for the rutile phase and 30 nm for the anatase phase.

To find out how the additives affect the anatase–rutile transformation of TiO₂, the crystal structures of the phases were examined. The following relation determines the lattice parameters of the powder

$$d = \frac{a}{\sqrt{h^2 + k^2 + \frac{a^2}{c^2}l^2}}, \quad (3)$$

where a and c are the lattice parameters, h, k, l are the Miller indices, and $d = d_{hkl}$ is the interplanar distance for the crystal. It can be seen in Table II that the lattice parameters of rutile and anatase phases do not change significantly for TiO₂ in the pure state and with additives.

Because of the low intensity of the peaks obtained for rutile TiO₂ with HCl and HF, we could not calculate the lattice parameters.

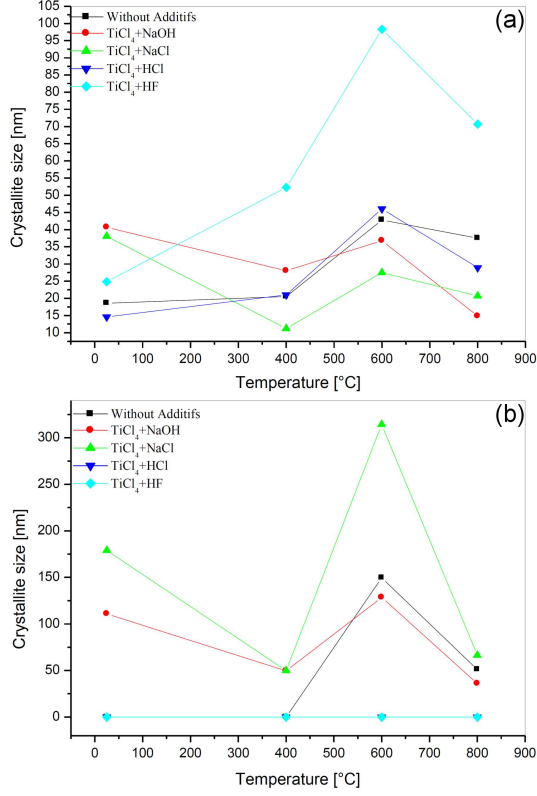


Fig. 3. Variation of average crystallite size with annealing temperature for anatase (a) and rutile (b) phases.

TABLE II

The lattice parameters of the samples of TiO_2 in the pure state and with additives annealed at 800°C for 1 h. The unit of all values is angstrom [\AA].

Phase	Anatase		Rutile	
	<i>a</i>	<i>c</i>	<i>a</i>	<i>c</i>
without additives	—	—	4.592	2.956
NaOH	3.911	9.462	4.608	2.926
NaCl	3.766	9.519	4.604	2.929
HCl	3.778	9.499	—	—
HF	3.774	9.501	—	—

Raman spectroscopy was used as a second technique to confirm the results obtained by XRD. The frequency of the Raman bands of anatase is located at 144 cm^{-1} with a strong signal, followed by low intensity peaks located at 197 , 399 , 513 , 519 , and 641 cm^{-1} . Meanwhile, the rutile phase has four Raman active modes appearing at 143 , 236 , 447 , and 613 cm^{-1} . Figure 4 shows the Raman spectra of TiO_2 powders with a proportion of rutile of 0, 57, and 93%, estimated by XRD. These three spectra are dominated by anatase peaks, which are more intense than the rutile ones. The sample with 93% of rutile phase presents two peaks at 477 and 613 cm^{-1} . The intensity of the 447 peaks is

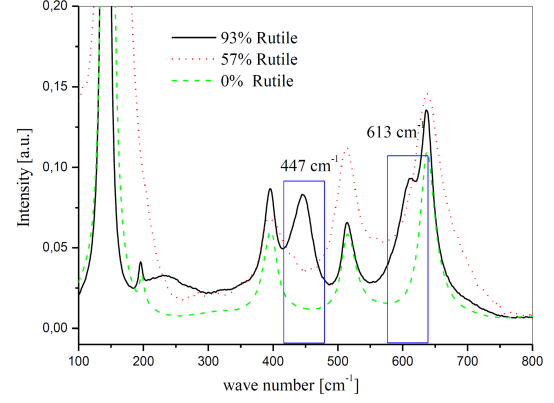


Fig. 4. Raman spectra of samples with different proportions of rutile.

comparable to the intensity of the 399 cm^{-1} anatase peak, while the 613 cm^{-1} peak of rutile phase is similar to 641 cm^{-1} anatase peak. In sample with 57% rutile, the 447 cm^{-1} peak appears as a weak shoulder. The green spectrum is pure anatase. Raman spectroscopy has been shown to be more sensitive for the analysis of samples even at the low contribution from anatase in the mixture powder.

The composition of the samples is deduced using the formula from the literature [21], namely

$$\frac{W_A}{W_R} = \frac{1}{16.37} \left(\frac{I_{A144}}{I_{R613}} - 1.37 \right) \left(\frac{W_A}{W_R} < 1 \right), \quad (4)$$

$$\frac{W_A}{W_R} = \left(\frac{I_{A399}}{I_{R447}} - 0.33 \right) \left(\frac{W_A}{W_R} > 1 \right), \quad (5)$$

where $\frac{I_{A144}}{I_{R613}}$ corresponds to the relative intensity of the case of low anatase content, and $\frac{I_{A399}}{I_{R447}}$ of the case of high anatase content. Then the relative intensity is plotted as a function of the ratio W_A/W_R , where W_A and W_R are the mass fraction of anatase and rutile, respectively. By having the value of W_A/W_R determined from the plot and knowing that $W_A + W_R = 1$, the percentage of each phase can be determined. The percentage of rutile calculated from XRD as a function of the percentage calculated from Raman spectroscopy is presented in Fig. 5. The function is linear, and the increase of the rutile concentration determined by XRD leads to a rutile increase estimated by Raman. We detect rutile in Raman when it is observed by XRD. The fractions of the rutile phase deduced by Raman are all weaker. XRD is has been shown to be more sensitive than Raman spectroscopy for detecting the rutile phase.

In order to verify the role of dissolved ions of additives in changing the morphology of particles, Fig. 6 shows the SEM images of TiO_2 powders synthesized: (panel a) at room temperature, (panel b) calcined at 800°C , (panel c) with the addition of HCl at 600°C , and (panel d) with the addition of NaOH at room temperature. SEM images suggest the formation of spherical agglomerates connected

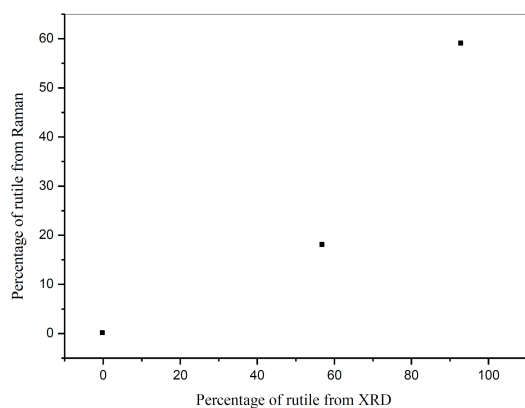


Fig. 5. Percentage change of rutile calculated from XRD in relation to the percentage calculated from Raman spectroscopy.

to each other, having a size of the order of μm . These agglomerates consist of smaller particles, the size of which increases with the annealing temperature (see Fig. 6a and b). It was also found that the pH of the solution affects the phase formation, structural morphology, and size. The size of the agglomerates is smaller for the sample obtained with the addition of HCl and having a pH of -1.5 (see Fig. 6c). On the other hand, the formation of agglomerates and small particles of irregular size begins upon reaction of the solution prepared with NaOH (PH= 13.5). The increase in agglomerates is attributed to the increasing concentration of H^+ , which promotes the neutralization of charged particles and therefore their agglomeration by the force of van der Waals [22]. The results show that the addition of Na^+ ions leads to a spherical morphology (see Fig. 6d). It has been shown in the literature that acidic, alkaline media and the strong repulsive charge between particles reduce the probability of coalescence, and a more stable sol can be formed. Studies by Su et al. [23] have indicated that the isoelectric of TiO_2 powder varies between the pH ranges of 5–6.8.

The photoactivity of TiO_2 was investigated using methylene blue (MB) as the representative pollutant. The photocatalytic degradation of methylene blue can be attributed to the hydroxyl radicals $\bullet\text{OH}$. These radicals are formed by the reaction between adsorbed OH^- on the TiO_2 surface and the holes h^+ on the valence band. Adsorption of MB on the surface of TiO_2 did not occur in all cases. Figure 7 shows the results of photocatalytic activity on the samples of TiO_2 prepared with the addition of NaOH, NaCl, HCl, and HF and calcined at 600°C . The optimal annealing temperature of about 500°C [24] or 600°C [25] was proposed so that sol-gel TiO_2 films have maximum photocatalytic activity. The photocatalytic activity of TiO_2 prepared with the NaOH additive was better than that of the samples prepared with the other additives. This

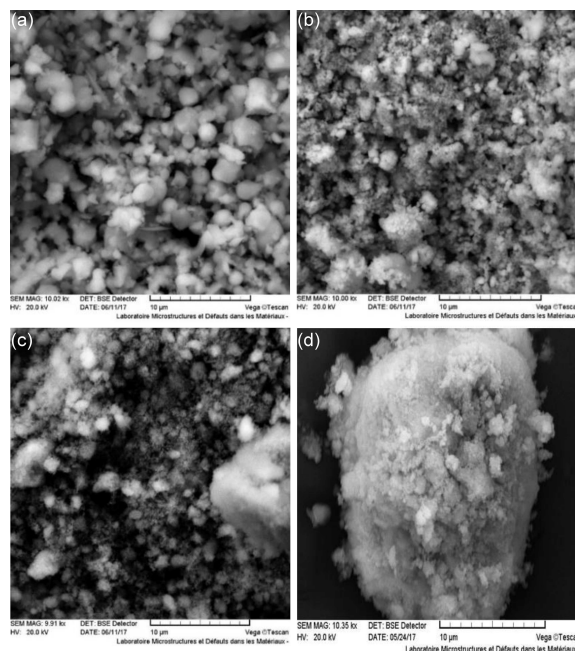


Fig. 6. Effect of different additives on morphology. SEM micrographs of synthesized TiO_2 powders: (a) TiO_2 at room temperature, (b) TiO_2 calcined at 800°C , (c) TiO_2 with addition of HCl at 600°C , and (d) TiO_2 with addition of NaOH at room temperature.

additive contributed to an increase in the number of hydroxyl radicals $\bullet\text{OH}$ on the TiO_2 surface, and therefore to an increase in the kinetics degradation. Na^+ in the TiO_2 films may affect the photocatalytic activity by changing the particle size [26], and low Na^+ content promotes high photocatalytic activity [27]. In the solution with a low concentration of Na^+ , there is an increase in OH^- ions, which induces good photocatalytic activity. If this concentration exceeds a threshold, their adsorption on the surface has the effect of countering the TiO_2 photoactivity. The sample with NaOH additive was a biphasic TiO_2 (anatase/rutile mixture) and contained 83% of the rutile phase at 600°C . However, Ohno et al. [28] reported that the sample containing a higher rutile fraction in the mixed crystalline phases generated better photoactivity in the discoloration test, compared to pure anatase or pure rutile powder. The photocatalytic behavior was explained on the basis of morphological characteristics. These results suggest that the photocatalytic of an anatase/rutile mixture is more effective for the degradation of methylene blue. It was indicated in the literature that the pH value affects the photocatalytic degradation of the organic pollutants in aqueous TiO_2 suspensions, which is variable and controversial [29]. It is well shown that the photodegradation degree increases with the decrease of pH. Our results show a good photocatalytic activity for the solution of samples with NaOH additives that has a pH = 9.1. This can be related to the

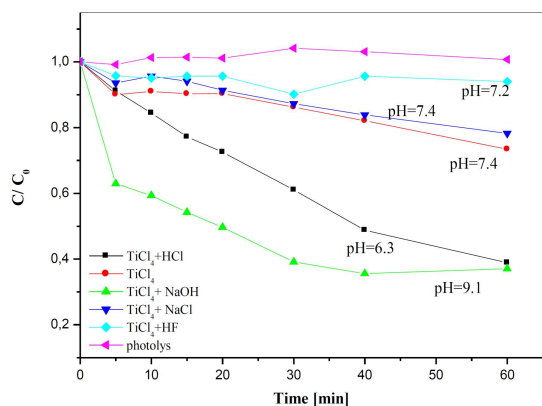
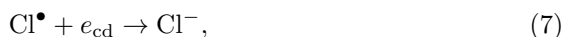


Fig. 7. Comparison of the photocatalytic degradation of MB in the presence of titania powder with different additives.

increase of OH^- ion concentration in this kind of solution. Since methylene blue (MB) has a cationic configuration, its adsorption was favored in alkaline [30]. At basic pH, the degradation rate is high, with a rapid change in the color of the solution. The degradation kinetics indicating the photolysis of MB is improved by the acid pH of the solution, which is shown in the case of samples prepared with HCl. Therefore, the photocatalytic activity of photocatalytic TiO_2 prepared with HCl additive was good despite containing 100% anatase. For solutions with a pH of around 7, the degradation rate is slow in the case of samples prepared by the addition of NaCl and HF. The presence of Cl^- contributes to trapping $\bullet\text{OH}$ radicals by adsorption on the TiO_2 surface and the formation of TiCl and H_2O , which induces $\bullet\text{OH}$ radicals reduction and decreases the photodegradation degree in the presence of NaCl [31]. The following reactions



describe the whole process. The same mechanism explains the behavior of the sample prepared with HF.

In other studies, it was observed that the rate increased with an increase in pH, exhibiting a maximum around pH of 6.9–8.0 [32]. The surface state of the metal oxide surface has a considerable influence on the photocatalytic activity with varying pH. The pH effect can be explained based on the zero point of charge of TiO_2 .

4. Conclusions

Nanocrystalline anatase TiO_2 has been successfully prepared by the sol-gel method. The XRD analysis shows that the anatase to rutile transformation of TiO_2 powder occurs at 600°C . At this

temperature, the crystallite size is at the maximum for both the anatase and rutile phases. The transformation is influenced by the presence of additives. It can begin at a low temperature and at room temperature when NaCl and/or NaOH are added to TiO_2 powder. Sodium contributes to accelerating the appearance of rutile at high fractions. However, when HCl and/or HF is added, the transition from anatase to rutile is delayed. On the other hand, additives modify the pH of the solution and the size of spherical agglomerates made of crystalline nanoparticles. A more acidic solution leads to smaller agglomerates, while solutions that are more basic give larger agglomerates, which have a size of a few micrometers. Photodegradation experiments indicated that the sample comprises $\approx 90\%$ of the rutile phase and has a higher photocatalytic activity. In the case of photocatalytic, TiO_2 is prepared with NaOH additives, which is the basic MB solution. It was also discovered that the photocatalytic activity is better in TiO_2 prepared with HCl, which is pure anatase and acid MB solution aqueous.

References

- [1] Z. Xu, L. Manhong, Z. Yongfa, *Thin Solid Films*. **515**, 7127 (2007).
- [2] J. Jiang, *Particuology*. **9**, 222 (2011).
- [3] G.K. Mor, M.A. Carvalho, O.K. Varghese M.V. Pishko, C.A. Grimes, *J. Mater. Res.* **19**, 628 (2004).
- [4] Chunlan Cao, Chenguo Hu, Xue Wang, Shuxia Wang, Yongshu Tian, Hulin Zhang, *Sens. Actuators B* **156**, 114 (2011).
- [5] M.S. Nahar, J. Zhang, K. Hasegawa, S. Kagaya, S. Kuroda, *Mater. Sci. Semicond. Process.* **12**, 168 (2009).
- [6] O. Carp, C. L. Huisman, A. Reller, *Prog. Solid State Chem.* **32**, 33 (2004).
- [7] K.E. Karakitsou, X.E. Verykios, *J. Phys. Chem.* **97**, 1184 (1993).
- [8] T. Ohno, K. Sarukawa, M. Matsumura, *J. Phys. Chem. B* **105**, 2417 (2001).
- [9] Y. Sakatani, D. Grosso, L. Nicole, C. Boissière, G.J. de A.A. Soler-Illia, C. Sanchez, *J. Mater. Chem.* **16**, 77 (2006).
- [10] N. Masahashi, Y. Mizukoshi, S. Semboshi, N. Ohtsue, *Appl. Catal. B* **90**, 255 (2009).
- [11] Huaiyong Zhu, Xueping Gao, Ying Lan, Deying Song, Yingxin Xi, Jincai Zhao, *J. Am. Chem. Soc.* **126**, 838 (2004).
- [12] C. Suresh, V. Biju, P. Mukundan, K.G.K. Warrier, *Polyhedron* **17**, 3131 (1998).
- [13] Q. Zhang, L. Gao, J. Guo, *Appl. Catal. B* **26**, 207 (2000).
- [14] Y. Hu, H.L. Tsai, C.L. Huang, *J. Eur. Ceram. Soc.* **23**, 691 (2003).

- [15] N. Nolan, S. Pillai, M. Seery, *J. Phys. Chem. C* **113**, 16151 (2009).
- [16] D.A.H. Hanaor, C.C. Sorrell, *J. Mater. Sci.* **46**, 855 (2011).
- [17] J.C. Yu, Jiaguo Yu, Wingkei Ho, Zitao Jiang, Lizhi Zhang, *Chem. Mater.* **14**, 3808 (2002).
- [18] Y. Takahashi, Y. Matsuoka, *J. Mater. Sci.* **23**, 2259 (1988).
- [19] W. Qin, J.A. Szpunar, *Phil. Mag. Lett.* **85**, 649 (2005).
- [20] H.M. Moghaddam, S. Nasirian, *Nanosci. Methods* **1**, 201 (2012).
- [21] V.H. Castrejon-Sanchez, E. Camps, M. Camacho-Lopez, *Superf. y Vacío* **27**, 88 (2014).
- [22] D.W. Kim, J.U. Kim, S.S. Shin, J.Y. Cho I.S. Cho, *J. Alloys Compd.* **697**, 222 (2017).
- [23] C. Su, B.Y. Hong, C.M. Tseng, *Catal. Today* **96**, 119 (2004).
- [24] Y. Tanaka, M. Suganuma, *J. Sol-Gel Sci. Technol.* **22**, 83 (2001).
- [25] Qi Xiao, Jiang Zhang, Chong Xiao, Zhichun Si, Xiaoke Tan, *Solar energy* **82**, 706 (2008).
- [26] H.J. Nam, T. Amemiya, M. Murabayashi, K. Itoh, *J. Phys. Chem. B* **108**, 8254 (2004).
- [27] N.A. Eleburuiké, W.A.W.A. Bakar, R. Ali, *Mal. J. Fund. Appl. Sci.* **13**, 143 (2017).
- [28] T. Ohno, K. Tokieda, S. Higashida, M. Matsumura, *Appl. Catal. A* **244**, 383 (2003).
- [29] Huaming Yang, Ke Zhang, Rongrong Shi, Xianwei Li, Xiaodan Dong, Yongmei Yu, *J. Alloys Compd.* **413**, 302 (2006).
- [30] Qi Xiao, Jiang Zhang, Chong Xiao, Zhichun Si, Xiaoke Tan, *Solar Energy* **82**, 706 (2008).
- [31] Yuexiang Li, Fang He, Shaoqin Peng, Dan Gao, Gongxuan Lu, Shuben Li, *J. Mol. Catal. A: Chem.* **341**, 71 (2011).
- [32] S. Lakshmia, R. Renganathan, S. Fujita, *J. Photochem. Photobiol. A: Chem* **88**, 163 (1995).